RSC Advances

Accepted Manuscript

This article can be cited before page numbers have been issued, to do this please use: S. Rakshit, S. Ghosh, S. Chall, S. S. Mati, S. P. Moulik and S. C. Bhattacharya, *RSC Adv.*, 2013, DOI: 10.1039/C3RA42628A.

Journal Name

RSC Advances

Dynamic Article Links ►
View Article Online
DOI: 10.1039/C3RA42628A

Cite this: DOI: 10.1039/c0xx00000x

www.rsc.org/xxxxxx

ARTICLE TYPE

Controlled Synthesis of Spin Glass Nickel Oxide Nanoparticles and Evaluation of their Potential Antimicrobial Activity: A Cost Effective and Eco Friendly Approach

Soumyadipta Rakshit,[a] Srabanti Ghosh,[b] Sayantani Chall,[a] Soumya Sundar Mati,[a] S.P.Moulik,[a,c] Subhash Chandra Bhattacharya,*[a,c]

Received (in XXX, XXX) Xth XXXXXXXXX 20XX, Accepted Xth XXXXXXXXX 20XX
DOI: 10.1039/b000000x

Development of an easy sustainable synthetic pathway towards oxide nanomaterials (NMs) is a necessary challenge for nanotechnology research workers. Additionally, antimicrobial activity of oxide nanoparticles against multi drug resistance pathogenic bacteria motivates scientists to focus their research on oxide materials. We report here a cost effective, simple and eco-friendly pathway of synthesizing NiO nanoparticles (NPs). X-ray diffraction and energy dispersive X-ray study confirmed their crystallinity and composition. Field emission scanning electron microscope (FESEM) was employed to understand their surface architecture and the dimension of synthesized NiO NPs were found to be 20-30 nm from transmission electron microscope (TEM) study. The as synthesized NiO demonstrated typical spin glass behaviour which is on advantage of our synthetic procedure. Antimicrobial properties of NiO NPs were investigated using gram negative and gram positive bacteria and their bactericidal effects were determined from minimum inhibitory concentrations (MIC) and Minimum bactericidal concentrations (MBC). Haemolytic activity revealed the nontoxic nature of the NPs towards the blood proteins at MBC. TEM images of bacteria cells treated with NiO NPs showed irreversible damages to the cell wall leading to cell death. In the light of our findings a possible mechanism of the antimicrobial effect of NiO NPs has been proposed.

Introduction

There is an unceasing pursuance in material science and chemistry to develop nanoscale materials having better performance with green approach due to environmental issues[1-5]. Since transitional metal oxides are key materials in catalysis, microelectronics, optical and magnetic applications their use in personal and commercial products is in a rush which necessitates greater insight towards their ecological impact (as they have intrinsic toxic property) on their release in environment[6-9]. Since insoluble metal oxide nanomaterials are expected to be more environmentally persistent, investigations on environmental perseverance, bioaccumulation and toxicity of these nanomaterials help to assess potential risks and provide information to industry to develop safer nanomaterials[10,12].

Owing to their specific functional characteristics and importance in a wide variety of technical applications, NiO nanoparticles have been investigated extensively as catalyst[13], electrode material for lithium ion batteries and fuel cells[14-16], in electrochromic films[17], electrochemical supercapacitors[18-19], magnetic materials[20] and gas sensors[21]. NiO is now also used for recyclable protein separation[22,23] and as biosensors[24]. Their increasing use in technology and biosystems motivated us to undertake this work.

Typically Nickel oxalates (NiOX) are potential precursors to produce NiO for their low cost, easy synthesis, good structure stability and low decomposition temperature. Different surfactants[25,26], sol-gel[27,28] methods as a soft chemistry route were used for controlled synthesis of NiO NPs. Even though these procedures have the ability to produce highly crystalline and uniformly sized NPs, they are not without drawbacks since these methods require expensive and toxic reagents and complicated synthetic steps. Therefore, the development of a simple, versatile and environment friendly method for the controlled synthesis of metal oxide NPs is required, not only for its fascinating utilization but also for the demand of time. Nevertheless, it has been reported that cellulose fibers[29], appoferritin[30], mammalian protein cages[31], viral protein cages[32] are effective materials for bio-templated preparation of oxide NPs.

Amid the diverse synthetic methodologies, we choose sol-gel technology since it is an impressive versatile approach for its important applications in practice. Use of eco-friendly material in this method makes it potential for different biomedical processes like enzyme, protein and antibody immobilization[33-36], entrapping of different drugs in porous matrices for therapeutic application[37], selective coatings for optical and electrochemical biosensors[38,39].

View Article Online
DOI: 10.1039/C3RA42628A

Bio gel derived nanoparticles show a very slow degree of release of bio-active agents[40]. Bio-gel templated synthesis route is an effective route towards metal oxide NPs. Though the major problem of the gel mediated synthesis is to control the reaction rates (which are generally too fast), resulting in formation of precipitates with a high degree of structural disorder, the bio-gel composed of APSA-80, Isopropyl myristate (IPM) and metal salt solution is quite an exception to that. APSA-80 is used in agriculture as a dispersant for various fungicide, insecticides and herbicides and as well as it is a very good spreader, activator for herbicides for their ability to make water "wetter". It has the ability to enhance the activity of Limonine (a Citrus fruit extract) to control Mealybugs, scale insects, white flies and aphides. It is extensively used as spray adjuvant in agriculture and has merely any antimicrobial effect[41]. Its formulation with IPM, another eco-friendly material and water can be used as a more stabilised vehicle for field application of pesticides with a better sustainable environment effect and can be used as a green template for nanoparticle synthesis[42]. In this present work, we have used a green material APSA-80 as a template to develop a controlled, eco-friendly and cost-effective synthesis of NiO NPs. After proper characterization we have discussed their interesting magnetic property.

Antimicrobial agents are very important in water disinfection and medicine since they can locally kill bacteria or slow down their growth without being toxic to surrounding tissue. Although chemically modified natural compounds are mostly applied antibacterial agents, with their broad use and abuse such as antibiotic therapy, horizontal gene transfer by conjugation, transduction or transformation etc. but emergence of bacterial resistance to these drugs are becoming a major problem these days[43,44]. This has prompted the interest in inorganic metal oxides which can provide an alternative strategy to treat bacterial diseases.In this context, it is interesting to mention that metal oxides are very easy to handle and are considered more environment friendly as compared to many others currently used as biocides. Gram-positive *Bacillus subtilis*, *Bacillus anthrax* are quite harmful towards human health since they can cause brain inflammatory diseases such as meningitis and encephalitis and they also produce allergic sensitivity[45-47]. *Pseudomonas aeruginosa* is a heavy metal tolerant strain. It is mostly notorious for causing lung infections or pneumonia in patients with compromised immune systems. Patients who are hospitalized for extended periods are frequently infected by this organism and can cause malignant external otitis, endophthalmitis, endocarditis, meningitis, pneumonia, and septicaemia[48-50]. However, considering the significance of studying antimicrobial activity of oxide nanomaterials, reports on NiO nanomaterials are quite rare. Y-W Baek et al. and Z.Wang et al. reported MIC and MBC values using commercially available NiO NPs[19,51,52]. Haemolysis is the destruction of red blood cells resulting in the release of haemoglobin into the surrounding fluid and is a measure to evaluate the toxicity of a material towards human blood. Thus, haemolytic data of a particular nanoparticle is also very essential for their possible usability in biomedical application. But literature did not reveal any satisfying data concerning haemolytic effect of the NiO NPs or even it did not discussed how they affect the cell growth[53].

From this perspective, we have focussed our work on whether our synthesized NiO NPs can act as a promising antimicrobial agent by determining Minimum Inhibitory Concentration (MIC) and Minimum Bactericidal Concentration (MBC). We also investigated the haemolytic activity for understanding the influence of the nanomaterial on human health. In the light of our findings we tried to propose a possible mechanism of antimicrobial effect.

2. Marterials and Methods

2.1. Reagents and Materials

The precursor metal salts nickel (II) nitrate hexahydrate ($Ni(NO_3)_2$. $6H_2O$, 99.9%) and sodium oxalate ($Na_2C_2O_4$,98%) were purchased from E. Merck. IPM (Isopropyl myristate, ≥ 98%) and APSA-80 were obtained from SRL (India) and AMWAY (Mumbai, India) respectively. All the chemicals were used as received. Acetone of analytical grade used in this work was purchased from E.Merck and dried by standard procedure[54]. The water was treated with a Millipore-Q water purification system.

2.2. Synthesis of NiOX and NiO nanoparticles

All syntheses were performed under ambient atmospheric condition. To prepare NiO nanoparticles we opted for a two-step synthesis approach. In the first step, we prepared Nickel oxalate by templating a bio-gel consisting of APSA-80, IPM, Ni^{2+} and $C_2O_4^{2-}$. In a typical synthetic procedure we prepared two different solutions. The first one was composed of 20 ml APSA-80, 10 ml IPM, 8.8 ml Ni^{2+} and the other one of 20 ml APSA-80, 10 ml IPM, 8.8 ml $C_2O_4^{2-}$. The two solutions were mixed and stirred vigorously to form gel. The resulted gel was put for 3 hours for completion of formation of Nickel Oxalate. The gel comprised of APSA-80 and IPM was then dissolved by adding acetone in it. After dissolving the gel the product (NiOX) was centrifuged and washed for 6 times with acetone. The recovered NiOX was then heated to 450°C at an increasing heat rate of 2°C. The optimal annealing temperature was found from thermogravimetric measurements to ensure complete conversion of precursor oxalates to oxide. A synthesis scheme has been given in Fig S1.

2.3. Screening for antimicrobial activity

Antibacterial activity of the NiO was determined by agar-diffusion assay as described previously[55,56] against some of the pathogenic Gram-positive and Gram-negative bacteria. Bacterial strains were first grown in Mueller-Hinton broth (MHB) under shaking condition for 4 h at 37°C and after the incubation period 1 ml of culture was spread on Mueller-Hinton agar (MHA). The wells were made using sterile 6 mm cork borer in the inoculated MHA plate. The wells were filled with 50 µl (1mg/ml) of the samples of NiO and blanks (phosphate buffer). Zone diameter was measured after 24 h incubation at 37°C.

2.4. Determination of Minimum inhibitory concentration (MIC) and minimum bactericidal concentration (MBC)

The minimum inhibitory concentration (MIC) dictates the lowest concentration at which an anti-microbial agent will inhibit the growth of a microorganism[57]. Another related method is the minimum bactericidal concentration (MBC). This indicates the

View Article Online
DOI: 10.1039/C3RA42628A

lowest concentration at which 99.9% of bacteria are killed by the compound under investigation. The MBC is the lowest concentration of an anti-microbial agent that will restrict the growth of the organism when subcultured into antibiotic-free media. MIC and MBC of materials were determined using the broth micro dilution[58]. An inoculum of the microorganism was prepared from 24 h MHB cultures and suspensions were adjusted with turbidity equivalent to that of a 0.5 McFarland standard. Bacterial suspensions were further diluted to 1:10 in sterile MHB to obtain a final inoculum of 5×10^5 CFU/ml. A 20 µl aliquot of the sample was added. Plates were covered and incubated for 24 h in ambient air at 37°C. After incubation, minimum inhibitory concentrations (MIC) were read visually; all wells were plated to nutrient agar and incubated. The minimal bactericidal concentration (MBC) was defined as a 99.9% reduction in CFU from the starting inoculum after 24 h incubation interval.

2.5. Haemolytic activity

Haemolysis test was employed to determine cellular toxicity of the NiO nanoparticles as previously described[59]. The 100% haemolytic positive control was the buffer containing 1% Triton X-100. Varying concentrations of NiO (0–1000 µg/mL) were then incubated with 1% human red blood cell suspension for 1 h at 37°C. After 1 h incubation, the mixtures were ice-cooled and centrifuged for 10 min at 1000 rpm at 4°C. The percent haemolysis was determined by measuring the optical density of the released haemoglobin in the supernatant at 540 nm. The experiments were run in triplicate for each concentration of NiO and were repeated three times.

2.6. Measurement and Characterization

A field emission scanning electron microscope (FESEM, S4800, Hitachi) equipped with an energy-dispersive X-ray spectrum was applied to determine the surface morphology and chemical composition of the as-prepared samples. Particle sizes, shapes, and HRTEM characterization were carried out in a JEOL JEM-2100 with a tungsten filament at an accelerating voltage operated at 200 kV. X-Ray diffraction (XRD) spectra were taken in a Bruker AXS D-8 Advance diffractometer at a scanning rate of 2°min^{-1},using the Cu Kα radiation (λ = 1.5406 Å) at an accelerating voltage and the applied current were 40 kV and 40 mA. Thermogravimetric analysis was carried out using a Perkin-Elmer Pyris instrument from room temperature to 600°C with a heating rate of 10°C min^{-1}. Magnetic properties of Nickel Oxide were measured by a SQUID magnetometer [MPMS XL7, Quantum Design, USA]. The optical densities of released haemoglobin were recorded with a Shimadzu UV-1601 PC UV-Vis spectrophotometer using matched quartz cells of path length 1 cm. Surface charge of NiO NPs was measured by Malvern, Zetasizer Nano ZS90.

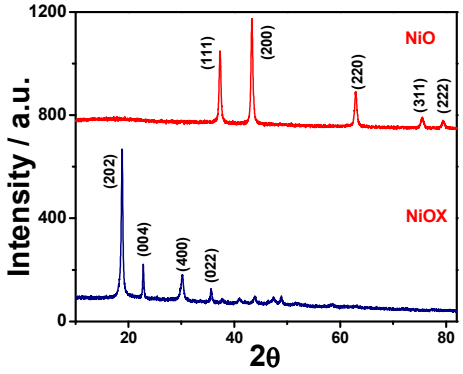

Figure 1: X-ray Diffraction pattern of as synthesized NiOX and NiO

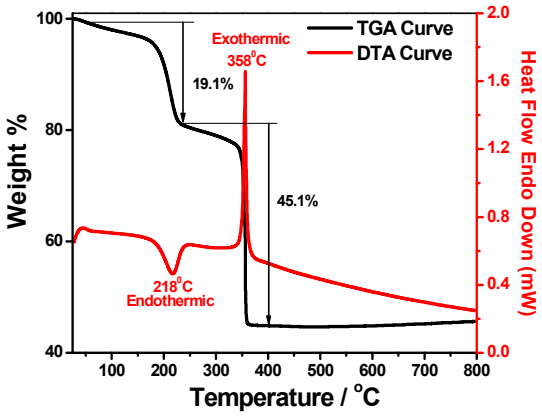

Figure 2: TGA-DTA plot of synthesized Nickel Oxalate precursor.

3. Results and Discussions

3.1. X-Ray Diffraction Analysis

The overall crystallinity and phase composition of the

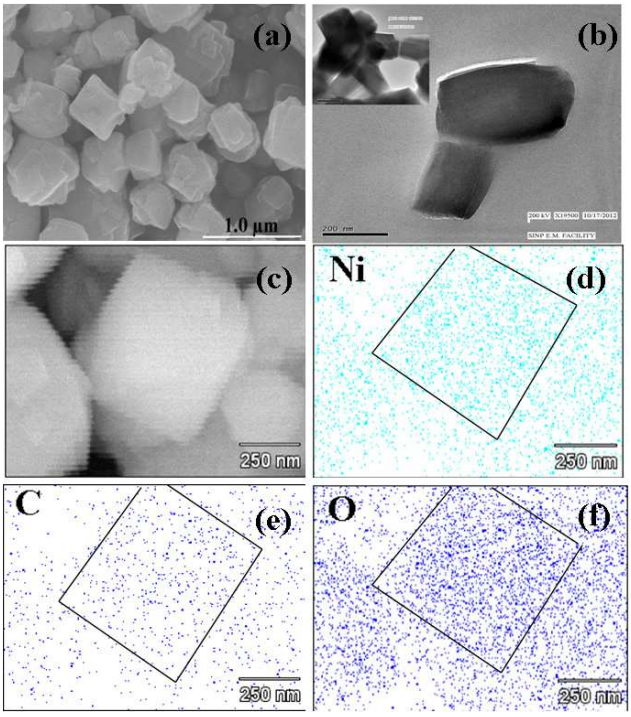

Figure 3: FESEM (a) and TEM (b) images of prepared Nickel Oxalate. (c) Shows a single NiOX NP and (d), (e), (f) show the elemental mapping of Ni, C, O respectively

View Article Online
DOI: 10.1039/C3RA42628A

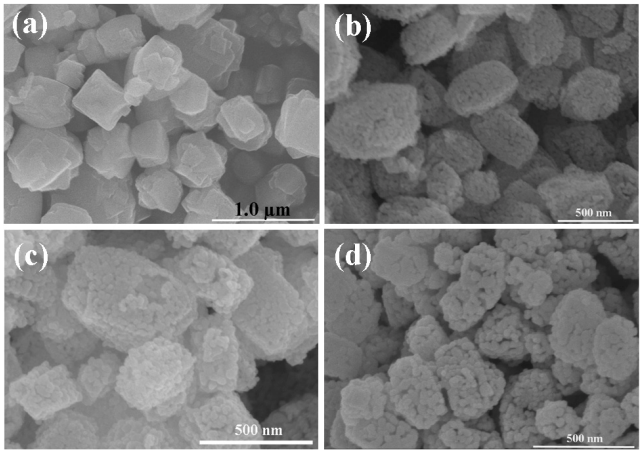

Figure 4: FESEM images indicating gradual degradation of NiOX NPs to NiO NPs at (a) 0 min (NiOX), (b) 60 minutes, (c) 120 minutes and (d) 180 minutes (NiO)

synthesized nanostructured NiOX and NiO were initially determined by X-ray Powder Diffractometer (XRD) and are shown in Figure 1. The XRD pattern of NiOX depicted in Figure 1 supported pure phase base centred orthorhombic NiOX (lattice parameters a= 11.84, b= 5.345, c= 15.716, Z= 8 and space group Cccm). The XRD pattern of NiO showed three major diffraction peaks and was indexed as (111), (200) and (220) crystal planes with a cubic structure which is in good agreement with literature value (JCPDS 78-0423). High intensity and broad spectral width in NiO XRD spectra affirmed their well grain size and detection of no other peak related to impurities further confirmed their high purity and crystallinity. Their compositions were further confirmed by EDX spectrometry (Figure S2 a, b)

3.2. Thermo Gravimetric Analysis

The TGA and DTA results of NiOX are presented in Figure 2. Two distinct weight loss steps in the temperature range 35 -240°C and 240 -380°C were observed. The first weight loss at 35–240°C corresponded to the exclusion of H_2O associated with an endothermic peak. The second weight loss at 240 -380°C was ascribed to the decomposition of oxalate. The exothermic peak associated with it clearly indicted loss of CO_2 molecule.

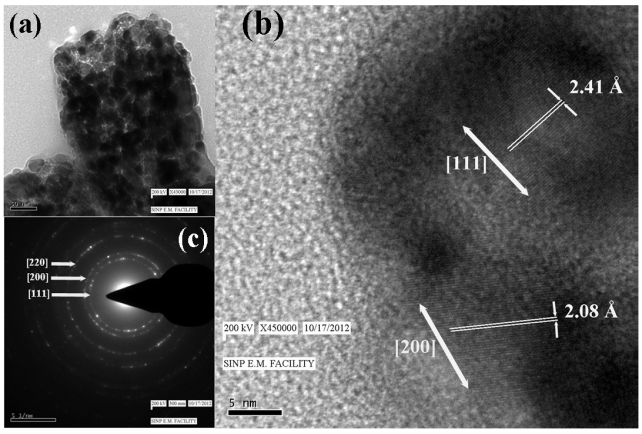

Figure 5: (a) TEM image of NiO obtained after calcination of NiOX. (b) is its HRTEM image showing inter planar distance 2.08Å and 2.41Å for [200] and [111] crystal planes respectively. (c) is the corresponding SAED pattern.

3.3. Electron Microscope Analysis (FESEM and TEM)

The morphology of Nickel Oxalate and Nickel Oxide nanoparticles was determined by FESEM. Figure 3a showed the typical FESEM images of Nickel Oxalate nanoparticles. The dimensions of NiOX NPs were found to be 0.4-0.5 µm and they were free of surface cracks and inter-structure adherence. TEM images of NiOX NPs also supported the observation.

In the elemental mapping Ni, C and O were found to be homogenously distributed in the synthesized NiOX NPs (Figure 3d, e, f) and that of Ni and O in NiO (Figure S3).

For a substantial view of the growth mechanism of NiO NPs, the time dependent evolution process was monitored. Figure 4

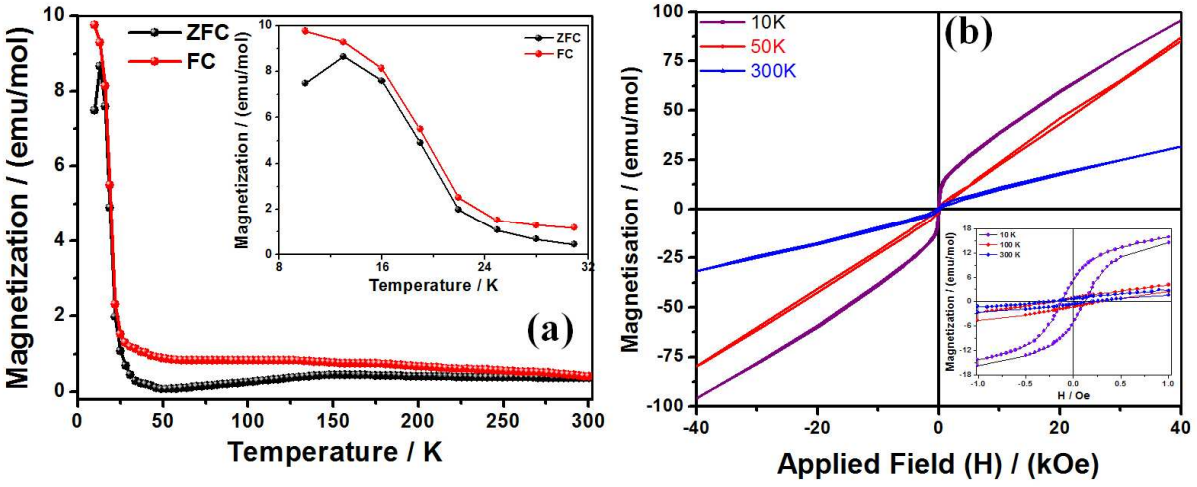

Figure 6: FC and ZFC magnetization curve for NiO (a) at an applied field 50 Oe. Inset shows ZFC and FC curves at the temperature region below 30K, where there is a cusp at ~13K. Hysteresis loops at 10K, 50K and 300K (b) and their magnification (inset of b).

View Article Online
DOI: 10.1039/C3RA42628A

(a,b,c,d) represents the FESEM images of the products that were obtained at different growth stages. The initial product Nickel oxalate when subjected to heat at 450°C at a heating rate 2°C min^{-1}, NiO nanoparticles (of smooth texture) were seen formed as surface cracks after 1 hr. But after 3 hrs their surfaces were found to be densely covered with small NiO NPs with dimension 20-30 nm. Their corresponding XRD patterns are also supported the observation (Fig S4). The HRTEM image of synthesised NiO clearly showed the distribution of NiO NPs within a parallelogram of dimension 20-30 nm (Figure S5). The close aggregation and packing of these NiO nanoparticles are shown in Fig. S3. A high-resolution TEM image (Figure 5b) displays clear lattices of NiO crystal, confirming the crystalline nature of NiO. The corresponding SAED pattern (Figure c) recorded on one NiO hollow microsphere suggests its polycrystalline nature. The diffraction rings can be easily indexed to the (220), (111), and (200) lattice planes of cubic NiO.

3.4. Magnetic Property

Magnetic properties of NiO were measured over a wide range of temperature and magnetic field. Temperature dependent magnetization curves (M-T) of synthesized NiO NPs were recorded under Field Cooling (FC) and Zero Field Cooling (ZFC) conditions from 10K to 300K at an applied field of 50 Oe. The results are shown in Figure 6a. The main feature of the ZFC curve was having two maxima: i) a broad maximum centred at T_1~150K and ii) a very sharp maximum was observed at a low temperature T_2~13K along with a bifurcation between FC and ZFC curves around 220K, which corresponded to Néel transition and also marked the largest nanoparticle present. Above this Néel temperature, thermal motions destroyed the antiparallel arrangement, and the nanomaterial then became paramagnetic[60]. For M_{FC} curve, magnetization increased monotonically with decreasing temperature from 300 to 5 K. The spin-glass-like behavior indicated that a spin-frozen transition might exist at around 13 K[61]. The high temperature maximum is commonly associated with mean blocking temperature denoting progressive blocking of uncompensated magnetic moments of the particle core[62]. As temperature was decreased the uncompensated surface spins started to correlate and formed spin clusters at the particle surface inducing a strong inter-particle interaction which led to a sharp maximum at ~13 K[63].

To get a clear view of this interesting magnetic property hysteresis loops were measured at different temperatures (10K, 50K, and 300K). At 10K it showed a fine hysteresis loop with a remnant magnetization 5.6 emu mol^{-1} exhibiting typical ferromagnetic behavior whereas for 50K and 300K the values became small revealing a superparamagnetic character (Figure 6b). The high temperature paramagnetic behavior suggested obliteration of long-range antiferromagnetism ordering[64].

Table 1: Minimum inhibitory concentration (MIC) and minimum bactericidal concentration (MBC) of NiO against multi-drug-resistant strains

Materials	Antibacterial activity (µg/mL)					
	P. Aeruginosa			B. Subtilis		
	MIC 1µg/mL	MBC 1µg/mL	Zone of inhibition (mm)	MIC 1µg/mL	MBC 1µg/mL	Zone of inhibition (mm)
NiO	8	16	18	8	32	21

3.5. Antimicrobial Effect of NiO

The antimicrobial activity of NiO nanoparticles was investigated against gram negative and gram positive bacteria using well diffusion method. In an agar plate, NiO NPs were used as test material and phosphate buffer as negative control. The inhibition

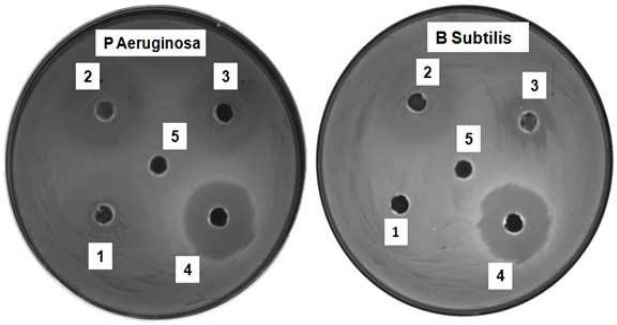

Figure 7: Determination of the effect of NiO nanoparticles on gram negative and gram positive bacteria by agar-diffusion assay method. *Pseudomonas aeruginosa* and *Bacillus subtilis* were spread on Agar plate. In each case, 1 represents Ni salt, 2, 3, 4 contains (8, 16, 32 µg/well), 5 represent 50 µl of water, were added to the wells.

zone formed in the screening test indicating the antimicrobial activity of NiO showed strong activity against both gram negative and gram positive bacteria such as *Pseudomonas aeruginosa* and *Bacillus subtilis* as evident from the clear zone of inhibition around the well containing this solution (as shown in Table 1 and Figure7). MIC (the lowest concentration at which no viable bacterial cell is present) against *Pseudomonas aeruginosa* and *Bacillus subtilis* was 8 µg/mL whereas the MBC values were 16 µg/mL and 32 µg/mL repectively. For better understanding antimicrobial effects of some other metal and metal oxide nanoparticles against these two bacteria are given in Table ST1.

Furthermore, our study aimed to unravel the cellular events that occurred upon exposure to NiO NPs with human blood cells in order to utilize them as antimicrobial agent. Figure 8 illustrates a

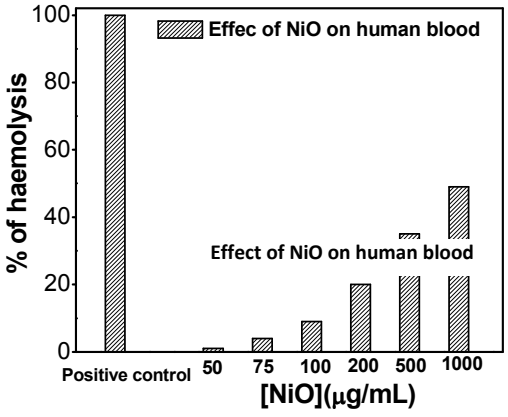

Figure 8: A dose–response plot for the haemolysis of human red blood cell in presence of NiO nanoparticles. In Haemolysis assay, Triton-X used as a positive control and red blood cells with different amount NiO nanoparticles.

View Article Online
DOI: 10.1039/C3RA42628A

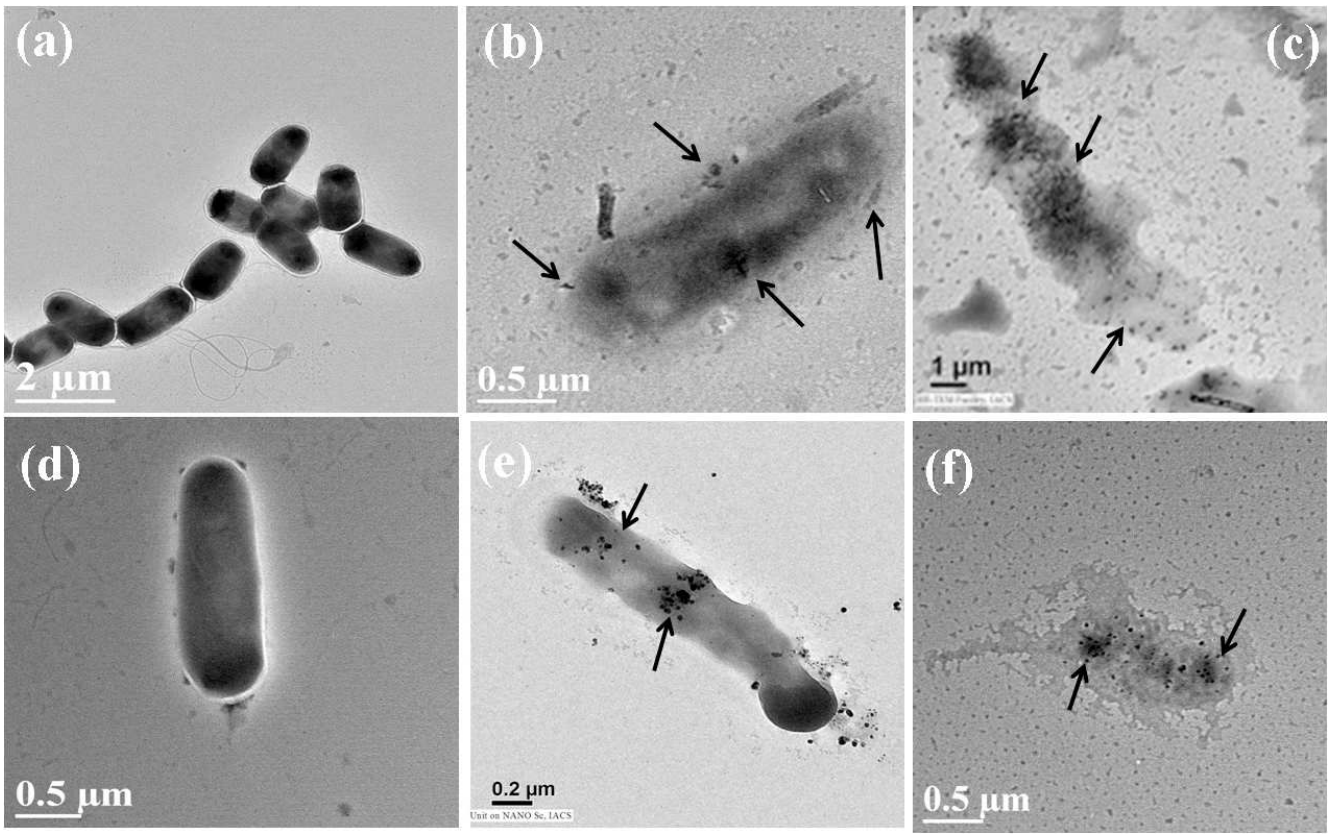

Figure 9: TEM images of *P. Aeruginosa* (a) control bacteria without nanoparticles treatment, treated with (b) MIC and (c) MBC of NiO nanoparticles. (d) *B. Subtilis* before treatment treated with (e) MIC and (f) MBC of NiO nanoparticles

dose–response profile of haemolysis of the red blood cells in presence of NiO. The haemolytic activity increased with increasing concentration of NiO nanoparticles while at MBC of NiO showed no haemolytic activity.

The haemolytic data suggested NiO has a strong affinity towards haemoglobin protein at higher concentration than MBC. The knowledge of the interaction of NiO with protein is crucial to address the engineering of NiO materials towards biocompatibility. Thus at a suitable concentration NiO (100 µg/mL) maintained the molecular structure of red blood cells without any toxicity.

To get an insight into the effect of NiO on bacteria, the morphologies of Gram-negative (*P. Aeruginosa*) and Gram-positive bacteria (*B. subtilis*) were examined by taking electron microscopic images before and after treatment with NiO nanoparticles at MIC and MBC. The incubation of bacteria with NiO for 2-3 h showed a significant change in their cell morphology. The TEM Micrographs of control *P. Aeruginosa* (Figure 9a) and *B. Subtilis* (Figure 9d) show relatively smooth cell surface compared to the treated cells with typical characters of rod shape. The TEM images revealed aggregation as well as alteration of cell morphology (Figure 9 b, c and e, f) on exposure to NiO nanoparticles.

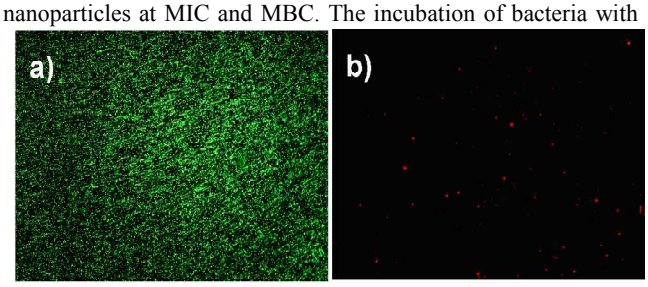

Figure 10: Fluorescence micrograph of *P. Aeruginosa* before (a) and after treating with NiO nanoparticles (b) in presence of LIVE/DEAD® BacLight TM Bacterial Viability Kit

The bacterial cells showed aberrant morphology with cracked and ruptured cell. The transmission electron microscopic studies revealed alteration of cellular morphology along with damage of the membrane on treatment with NiO NPs. The interaction between nanoparticle surface and the cell wall constituents might have caused structural changes and damage to the cellular membranes.

Outer Membrane of Gram-negative bacteria is composed of lipopolysaccharide in addition to a thin peptidoglycan layer and act as a primary permeability barrier for macromolecules and hydrophobic drugs. But for Gram-positive bacteria the structure is rather simple as they have a membrane, which surrounds the cell, and a cell wall primarily made up of peptidoglycan layer as well as teichoic and lipoteichoic acids[65]. Still date the mechanism of antimicrobial activity of NiO is not clear.

For both cases due to direct contact NiO NPs damaged the cell membrane. The global charge of the bacterial cell at physiological pH was negative due to the dissociation of excess carboxylic groups at the cell surface[66]. Since NiO has a positive surface charge and a $\zeta = 36.8 \pm 0.9$ mV (found from Zeta potential measurement), they became electrostatically bound to the

View Article Online
DOI: 10.1039/C3RA42628A

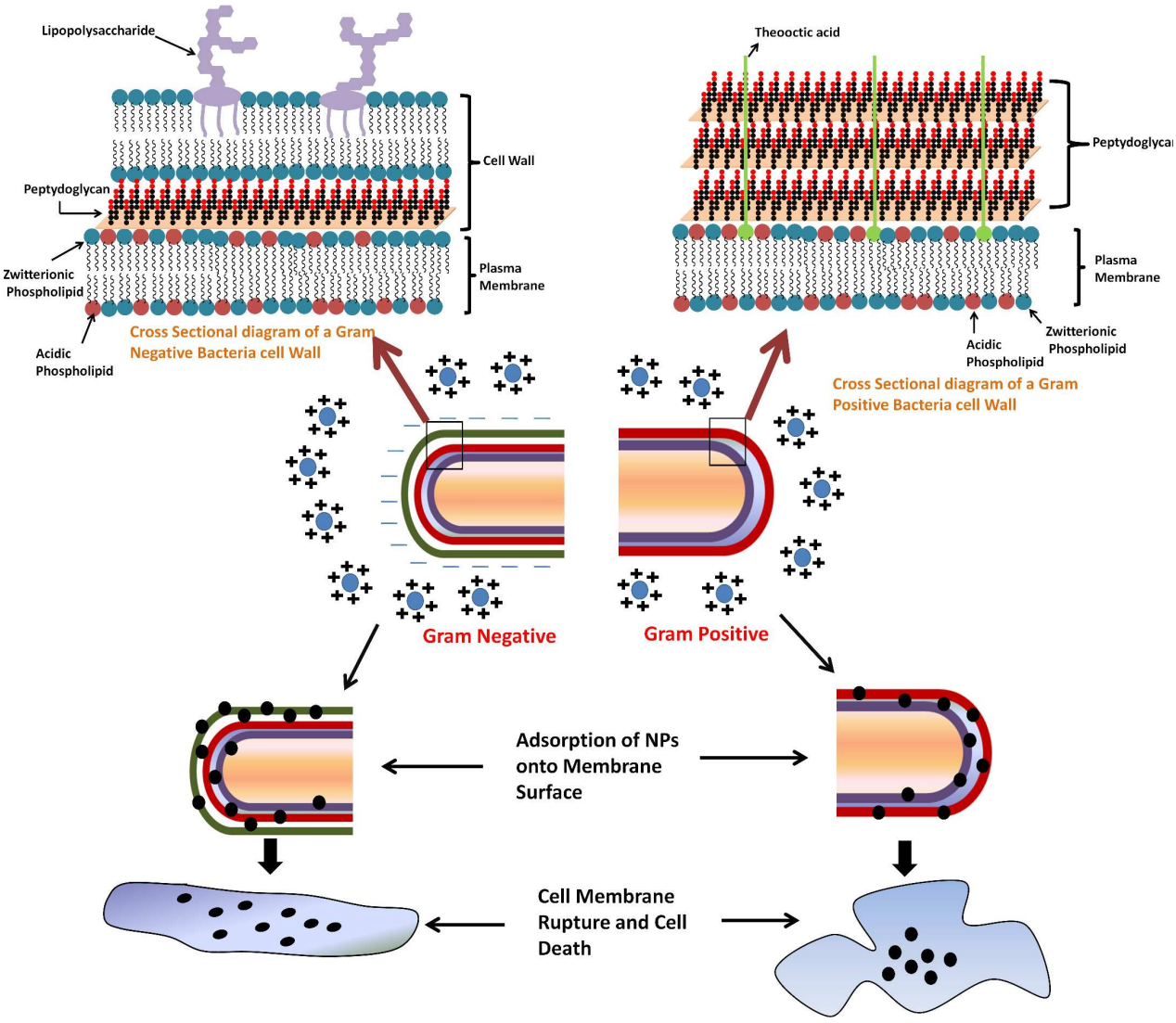

Scheme 1: Schematic representation of possible mechanism of antimicrobial activity of NiO NPs

negative cell surface hindering the cell activity. Penetration of NiO into the cell and its toxicity made it inactive and dead followed by lysis. The above process has been depicted in Scheme 1.

The antibacterial activity of the NiO nanoparticles was also followed by fluorescence microscopy using LIVE/DEAD® BacLightTM bacterial viability kit[67] The kit contains two nucleic acid binding stains, SYTO 9 and propidium iodide. These dyes have different cell penetration properties along with distinct spectral characteristics. SYTO 9 binds to the nucleic acid of both living and dead cells and exhibits green fluorescence after excitation with BP460–495 nm filter. Propidium iodide only binds to the nucleic acid of dead cells and shows red fluorescence. The fluorescence microscopic images of untreated Gram-negative, *P. Aeruginosa* and that of same bacterial cells treated with 16 µg/mL of NiO, respectively are shown in Figure10. All the untreated cells exhibited green fluorescence indicating the living status of bacteria. However, the observed red fluorescence in the microscopic image (Figure 10b) of NiO treated bacteria with propidium iodide further confirmed the bactericidal efficiency of the NiO nanoparticles.

Conclusion

In short we developed a simple, controllable and environment friendly bottom up pathway for synthesizing NiO nanoparticles which were characterised by means of XRD, FESEM and TEM. Magnetic study indicated their spin glass behaviour. The broad spectrum of antimicrobial activity of these NiO nanoparticles with low MIC values clearly indicated their efficiency towards inhibiting the growth of gram positive and gram negative bacteria. TEM pictures of the bacteria treated with NiO NPs indicated that the antimicrobial action was governed via membrane disruption and cell lysis and may be stable positive surface charge played a vital role in it. Their low haemolytic activity at bactericidal concentration further makes them useful for biomedical application. For its easy preparation, low cost, high abundance and excellent bactericidal effect, NiO has a promising role for future antibacterial agent.

View Article Online
DOI: 10.1039/C3RA42628A

Acknowledgement

Authors S.R and S.S.M acknowledge UGC for providing JRF and SRF. S.G. gratefully acknowledges CSIR for financial support. S.C., S.B and S.P.M greatly appreciate the funding from DST (SR/S1/PC-63/2009). SPM also thanks INSA for support. S.R acknowledges Mr. I. Mukherjee for his help in preparing gel by APSA-80. Authors are grateful to Dr. K. K. Chattopadhyay, Mr. N.S. Das and Mr. D. Sarkar of Jadavpur University for their kind help in doing TEM and FESEM measurement. Help of Mr. Pulak Ray of SINP in TEM measurements is also greatly acknowledged.

Notes and references

[a] *Department of Chemistry, Jadavpur University, Jadavpur, Kolkata-700032, India. Fax: 91(033) 24146584; Tel: 033 2414 6223; E-mail: sbjuchem@yahoo.com, scbhattacharyya@chemistry.jdvu.ac.in*
[b] *Centre for Advanced Materials, Indian Association for the Cultivation of Science, Jadavpur, Kolkata-700032, India.*
[c] *Centre for Surface Science, Department of Chemistry, Jadavpur University, Jadavpur, Kolkata-700032*

† Electronic Supplementary Information (ESI) available: [Scheme of Synthesis of NiO Nanoparticles, Energy dispersive X-ray spectrum of NiOX and NiO Nanoparticles, Elemental Mapping of Ni and O in NiO, Nickel Oxalate parallelograms and distribution of NiO NPs within the parallelogram, Summary of select studies concerning the antimicrobial effects of other metal and metal oxide nanoparticles have been included]. See DOI: 10.1039/b000000x/

1 Z. Marková, K. Šišková, J. Filip, K. Šafářová, R. Prucek, A. Panáček, M. Kolářb and R. Zbořil, *Green Chem*, 2012, **14**, 2550
2 Y. Zhang, X. Wang, L. Zeng, S. Songb and D. Liu *Dalton Trans*., 2012, **41**, 4316
3 A. P. Bhirud, S. D. Sathaye, R. P. Waichal, L. K. Nikam and B. B. Kale, *Green Chem.*, 2012, **14**, 2790
4 M. Baro, P. Nayak, T. T. Baby and S. Ramaprabhu, *J. Mater. Chem. A*., 2013, **1**, 482
5 P. Manjula, R. Boppella and S. V. Manorama, *ACS Appl. Mater. Interfaces.*, 2012, **4**, 6252
6 P. K. Stoimenov, R. L. Klinger, G. L. Marchin and K. J. Klabunde, *Langmuir,* 2002**, 18***,* 6679
7 Y. Hou, H. Kondoh, M. Shimojo, T. Kogure and T. Ohta, *J. Phys. Chem. B,* 2005, **109**,19094
8 X. Wang, X. Chen, L. Gao, H. Zheng, M. Ji, C. Tang, T. Shen and Z. Zhang, *J. Mater.Chem.*, 2004, **14**, 905.
9 F. Cai, G. Zhang, J. Chen, X. Gou, H. Liu and S. Dou, *Angew. Chem. Int. Ed.*, 2004, **43**, 4212
10 M. Li, S. Pokhrel, X. Jin, L. Mädler, R. Damoiseaux and E. M. V. Hoek, *Environ. Sci. Technol.*, 2011, **45**, 755
11 G. Applerot, R. Abu-Mukh, A. Irzh, J. Charmet, H. Keppner, E. Laux, G. Guibert and A. Gedanken, *ACS Appl. Mater. Interfaces.* 2010, **2**, 1052
12 N. L. Rosi and C. A. Mirkin, *Chem. Rev*., 2005, **105**, 1547
13 J. Park, E. Kang, S. U. Son, H. M. Park, M. K. Lee, J. Kim, K. W. Kim, H. J. Noh, J. H. Park, C. J. Bae, J. G. Park and T. Hyeon, *Ad*V. *Mater.*, 2005, **17**, 429
14 F. Cao, F. Zhang, R. Deng, W. Hu, D. Liu, S. Songa and H. Zhang, *CrystEngComm*., 2011, **13**, 4903
15 P. Poizot, S. Laruelle, S. Grugeon, L. Dupont and J.M. Tarascon, *Nature*, 2000, **407**, 496
16 X. Wang, L. Li, Y. G. Zhang, S. T. Wang, Z. D. Zhang, L. F. Fei and Y. T. Qian, *Cryst. Growth Des.*, 2006, **6**, 2163
17 M. C. A. Fantini, F. F. Ferreira and Gorenstein,A. *Solid State Ionics.*, 2002, **152-153**, 867
18 T. Ahmad, K. V. Ramanujachary, S. E. Lofland and A. K. Ganguli, *Solid State Sciences*, 2006, **8**, 425
19 H. Pang, Q. Lu, Y. Lia and F. Gao, *Chem. Commun*, 2009, 7542
20 S. D. Tiwari and K. P. Rajeev, *Thin Solid Films*., 2006, **505**, 113
21 X. Song, L. Gao and S. Mathur, *J. Phys. Chem. C*., 2011, **115**, 21730
22 I.S. Lee, N. Lee, J. Park, B.H. Kim, Y.W. Yi, T. Kim, T.K. Kim, I.H. Lee, S.R. Paik and T. Hyeon, *J. Am. Chem. Soc.*, 2006, **128**, 10658
23 J. Kim, Y. Piao, N. Lee, Y. Park, I.H. Lee, J.H. Lee, S.R. Paik and T. Hyeon,*AdV. Mater*., 2010, **22**, 57
24 S. Mohan, P. Srivastav, S. N. Maheshwari, S. Sundarb and R. Prakash, *Analyst*., 2011, **136**, 2845
25 S. Vaidya, P. Rastogi, S. Agarwal, S. K. Gupta, T. Ahmad, Jr., A. M. Antonelli, K. V. Ramanujachary, S. E. Lofland and A. K. Ganguli, *J. Phys. Chem. C*., 2008, **112**, 12610
26 S. Rakshit, S. Chall, S. S. Mati, A. Roychowdhury, S.P. Moulik and S. C. Bhattacharya, *RSC Adv.*, 2013,**3**, 6106
27 T. Sreethawong, S. Chavadej, S. Ngamsinlapasathian and S. Yoshikawa, *Colloids and Surfaces A: Physicochem. Eng. Aspects.*, 2007, **296***, 222*
28 D. G. Shchukin, J. H. Schattka, M. Antonietti and R. A. Caruso, *J. Phys. Chem. B.*, 2003, **107***,* 952
29 H. Dong and J. P. Hinestroza, *ACS Appl. Mater. Interfaces.*, 2009, **1(4)**, 797
30 K. Iwahori and I. Yamashita, *Journal of Cluster Science*., 2007, **18(2)**, 358
31 R. M. Kramer, C. Li, Carter, D. C. M. O. Stone and R. R. Naik*, J. Am. Chem. Soc.*, 2004, **126**, 13282
32 J. M. Slocik, R. R. Naik, M. O. Stone and D. W. Wright, *J. Mater. Chem.*, 2005, **15**, 749; C. Chen, M.C. Daniel, Z. T. Quinkert, M. De, B. Stein, V. D. Bowman, P. R. Chipman, V. M. Rotello, C. C. Kao and B. Dragnea, *Nano Lett.*, 2006, **6(4)**,611
33 A.P. Chiriac, I. Neamtu, L.E. Nita and M.T. Nistor, *Mini-Reviews in Medicinal Chemistr*, 2010*,* **10***,* 990
34 K.E. LeJeun, J.R. Wild and A.J. Russell, *Nature,* 1998, **395**, 27
35 I. Gill. *Chem. Mater.*, 2001, **13**, 3404
36 H.H. Yang, Q.Z. Zhu, H.Y. Qu, X.L. Chen, M.T. Ding and J.G. Xua, *Anal. Biochem*, 2002, **308**, 71
37 C. Barbé , J. Bartlett, L. Kong, K. Finnie, H. Q. Lin, M. Larkin, S. Calleja, A. Bush and G. Calleja, *Adv. Mater*, 2004, **16**, 1959
38 M.R.N. Monton, E. M. Forsberg and J. D. Brennan, *Chem Mater*, 2012, **24**, 796
39 Q. Wang, G. Lu and B. Yang, *Sens. Actuators B*, 2004, **99**, 50
40 S. Gulaim, V.G. Kessler, M. Unell and S. Håkansson, Proceeding of 1st International Conference on Nanostructured Materials and Nanocomposites, Kottayam, India, ICNM-2009, **135**
41 I. Mukherjee, D. Haldar, S. Ghosh and S.P. Moulik, *J. Disp. Sc and Tech*, 2009, **30**, 1430
42 G.R.. Hollingsworth, *J. Econ. Entomol*, 2005, **98(3)**, 772
43 M. J. Hajipour, K. M. Fromm, A. A. Ashkarran, D. J. de Aberasturi, I. R.de Larramendi, T. Rojo, V. Serpooshan, W.J. Parak and M. Mahmoudi, *Trends in Biotechnology*, 2012, **30 (10)**, 499
44 W. Witte, *Infect. Genet. Evol*. 2004, **4**, 187
45 C. Ewald, S. Kuhn and R. Kalff, *Neurosurg. Rev*, 2006, **29**, 163
46 F. Bert, O. Ouahes and N.L. Zechovsky, *J. Clin. Microbiol*, 1995, **33**, 1950
47 L. Liu, K. Xu, H. Wang, J.Tan P. K., W. Fan, S.S. Venkatraman, L. Li and Y.Y. Yang, *Nature Nanotechnology*, 2009, **4**, 457
48 Y. Yang, J. M. Mathieu, S. Chattopadhyay, J.T. Miller, T. Wu, T. Shibata, W. Guo and P. J. J. Alvarez, *ACS Nano*, 2012, **6**, 6091: C. K. Stover, X. Q. Pham, A. L. Erwin, S. D. Mizoguchi, P. Warrener, M. J. Hickey, F. S. L. Brinkman, W. O. Hufnagle, D. J. Kowalik, M. Lagrou, et al., *Nature*, 2000, **406**, 959
49 V. Balloy, A. Verma, S. Kuravi, M. S. Tahar, M. Chignard and R. Ramphal, *J Infect Dis*, 2007, **196**, 289
50 J. Rello, P. Jubert, J. Vallés, A. Artigas, M. Rué and M. S. Niederman, *Clin Infect Dis*, 1996 , **23**, 973
51 Y.W. Baek and Y.J. An, *Science of the Total Environment*, 2011, **409**, 1603
52 Z. Wang, Y.H. Lee, B. Wu, A. Horst, Y. Kang, Y.J. Tang and D.R. Chen, *Chemosphere*, 2010, **80**, 525
53 N. Gonga, K. Shao, W. Fengc, Z. Lina, C. Lianga and Y. Suna, *Chemosphere*, 2011, **83**, 510
54 B. S. Furniss, A. J. Hannaford, P. W. G. Smith and A. R. Tatchell, Vogel's Text Book of Practical Organic Chemistry, *Longman Singapore Publishers Pte. Ltd.*, 1989, **5th Edition**, Singapore, 408

View Article Online
DOI: 10.1039/C3RA42628A

55 P. Thakurta, P. Bhowmik, S. Mukherjee, T. K. Hajra, A. Patra and P. K. Bag, *J. Ethnopharmacol*, 2007, **111**, 607

56 D. S. Reeves, P.M. Hawkey and D. A. Lewis (Eds), *Medical bacteriology: a practical approach,* IRL Press, Oxford, 1989, **Chapter 8**, 195

57 J. M. Andrews, *J. Antimicrob. Chemother*, 2001, **48**, 5

58 NCCLS, "Methods for determining bactericidal activity of antimicrobial agents. Approved guideline M26-A" (1999) National Committee for Clinical Laboratory Standards, Wayne, Pa

59 H. Situ, and L. A. Bobek, *Antimicrob. Agents Chemother*, 2000, **44**, 1485

60 S. Thota and J. Kumar, Journal of Physics and Chemistry of Solids, 2007, **68**, 1951; M. P. Proenca, C.T. Sousa, A. M. Pereira, P. B. Tavares, J. Ventura, M. Vazquez and J. P. Araujo, *Phys. Chem. Chem. Phys.*, 2011, **13**, 9561

61 S.K. Sharma, J.M. Vargas, E. De Biasi, F. B´eron, M. Knobel, K. R. Pirota, C.T. Meneses, S. Kumar, C.G. Lee, P.G. Pagliuso and C. Rettori, *Nanotechnology*, 2010, **21,** 035602

62 F.H. Aragón, P.E.N. de Souza, J.A.H. Coaquira, P. Hidalgo and D. Gouvêa, *Physica B*, 2012, **407**, 2601

63 M. Y. Ge, L. Y. Han, U. Wiedwald, X. B. Xu, C. Wang, K. Kuepper, P. Ziemann and J. Z. Jiang, *Nanotechnology*. 2010, **21**, 425702; R. Das, A. Jaiswal, S. Adyanthaya and P. Poddar, *J. Phys. Chem. C*, 2010**, 114**, 12104

64 R. H. Kodama, S. A. Makhlouf and A. E. Berkowitz, *Phys. Rev. Lett*, 1997, **79**, 1393

65 P. J. P. Espitia, N. de F. F. Soares, J. S. dos R. Coimbra, N. J. de Andrade, R. S. Cruz and E. A. A. Medeiros, *Food Bioprocess Technol,* 2012, **5**,1447; A. M. Fayaz, K. Balaji, M. Girilal, R. Yadav, P. T. Kalaichelvan, R. Venketesan, *Nanomedicine: Nanotechnology, Biology, and Medicine*, 2010, **6**, 103

66 P. K. Stoimenov, R. L. Klinger, G. L. Marchin and K. J. Klabunde, *Langmuir*, 2002, **18**, 6679

67 L. Boulos, M. Prevost, B. Barbeau, J. Coallier and R. J. Desjardins, *Microbiol. Methods*, 1999, **37**, 77

View Article Online
DOI: 10.1039/C3RA42628A

Controlled Synthesis of Spin Glass Nickel Oxide Nanoparticles and Evaluation of their Potential Antimicrobial Activity: A Cost-Effective and Eco-Friendly Approach

Soumyadipta Rakshit [a], *Srabanti Ghosh* [b], *Sayantani Chall* [a], *Soumya Sundar Mati* [a], *S.P.Moulik* [ac], *Subhash Chandra Bhattacharya** [ac]

[a] Department of Chemistry, Jadavpur University, Kolkata -700032, India

[b] Centre for Advanced Materials, Indian Association for the Cultivation of Science, Jadavpur, Kolkata-700032, India

[c] Centre for Surface Science, Department of Chemistry, Jadavpur University, Kolkata -700032, India

*E-mail : sbjuchem@yahoo.com / scbhattacharyya@chemistry.jdvu.ac.in

*Phone No: 033 2414 6223; *Fax: 91(033) 24146584

Graphical Abstract

View Article Online
DOI: 10.1039/C3RA42628A

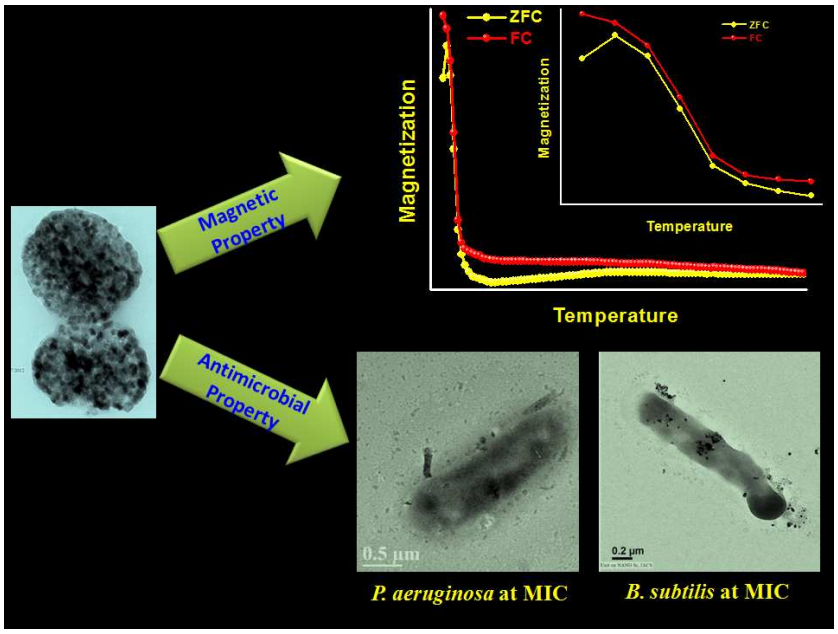

Magnetic Property of NiO depicting Spin Glass behavior and their antimicrobial effect on gram-positive and gram-negative bacteria